

PCCP

Accepted Manuscript



This is an *Accepted Manuscript*, which has been through the Royal Society of Chemistry peer review process and has been accepted for publication.

Accepted Manuscripts are published online shortly after acceptance, before technical editing, formatting and proof reading. Using this free service, authors can make their results available to the community, in citable form, before we publish the edited article. We will replace this *Accepted Manuscript* with the edited and formatted *Advance Article* as soon as it is available.

You can find more information about *Accepted Manuscripts* in the [Information for Authors](#).

Please note that technical editing may introduce minor changes to the text and/or graphics, which may alter content. The journal's standard [Terms & Conditions](#) and the [Ethical guidelines](#) still apply. In no event shall the Royal Society of Chemistry be held responsible for any errors or omissions in this *Accepted Manuscript* or any consequences arising from the use of any information it contains.

PCCP Guidelines for Referees

Physical Chemistry Chemical Physics (PCCP) is a high quality journal with a large international readership from many communities

Only very important, insightful and high-quality work should be recommended for publication in PCCP.



To be accepted in PCCP - a manuscript must report:

- Very high quality, reproducible new work
- **Important new physical insights** of significant general interest
- A novel, stand-alone contribution

Routine or incremental work should not be recommended for publication. Purely synthetic work is not suitable for PCCP

If you rate the article as 'routine' yet recommend acceptance, please give specific reasons in your report.

Less than 50% of articles sent for peer review are recommended for publication in PCCP. The current PCCP Impact Factor is 3.83

PCCP is proud to be a leading journal. We thank you very much for your help in evaluating this manuscript. Your advice as a referee is greatly appreciated.

With our best wishes,

Philip Earis (pccp@rsc.org)
Managing Editor, PCCP

Prof Daniella Goldfarb
Chair, PCCP Editorial Board

General Guidance (For further details, see the RSC's [Refereeing Procedure and Policy](#))

Referees have the responsibility to treat the manuscript as confidential. Please be aware of our [Ethical Guidelines](#) which contain full information on the responsibilities of referees and authors.

When preparing your report, please:

- Comment on the originality, importance, impact and scientific reliability of the work;
- State clearly whether you would like to see the paper accepted or rejected and give detailed comments (with references) that will both help the Editor to make a decision on the paper and the authors to improve it;

Please inform the Editor if:

- There is a conflict of interest;
- There is a significant part of the work which you cannot referee with confidence;
- If the work, or a significant part of the work, has previously been published, including online publication, or if the work represents part of an unduly fragmented investigation.

When submitting your report, please:

- Provide your report rapidly and within the specified deadline, or inform the Editor immediately if you cannot do so.
- We welcome suggestions of alternative referees.

ARTICLE

Amyloid- β (1-40) restores adhesion properties of pulmonary surfactant, counteracting the effect of cholesterol

Cite this: DOI: 10.1039/x0xx00000x

Received 00th January 2012,
Accepted 00th January 2012

DOI: 10.1039/x0xx00000x

www.rsc.org/

F.T. Hane^a, E. Drolle^{a,b}, Z. Leonenko^{a, b, c}

Pulmonary surfactant (PS) is a thin lipid-protein film covering the surface of the lung alveoli at the air/liquid interface. The primary purpose of PS is to control the surface tension of the air/liquid interface and to reduce the work of breathing. High levels of cholesterol in PS are associated with life-threatening acute respiratory distress syndrome (ARDS) and acute lung injury (ALI). Finding therapeutics to counteract the effect of cholesterol in PS is a matter of contemporary research.

In our earlier work, we showed that the addition of amyloid- β (1-40) (A β 40), the protein implicated in Alzheimer's disease, can reverse the detrimental effects of cholesterol in surfactants by improving multilayer formation and restoring PS surface active properties. We hypothesized that this phenomenon was due to A β 40 improving adhesion properties of surfactant. In this work we used atomic force spectroscopy to demonstrate that A β 40 counteracts the adhesive properties of PS compromised by high levels of cholesterol in PS and helps to restore the functionality of PS.

Keywords: pulmonary surfactant, BLES, Langmuir-Blodgett monolayer, amyloid- β , cholesterol, atomic force microscopy, atomic force spectroscopy, adhesion forces.

Introduction

Pulmonary Surfactant (PS) is a molecular film at the air/liquid interface of mammalian alveoli. PS has three essential functions necessary for respiration: a) rapid adsorption, b) reduction of surface tension on surfactant compression, and c) surfactant replenishment on expansion¹. At the end of expiration, PS reduces the surface tension of the air/liquid interface to levels approaching 0 mN/m to reduce the work required for breathing. During inspiration, the surface tension of PS increases to prevent alveolar collapse². The method by which pulmonary surfactant changes surface tension occurs through the dynamic exchange of surfactant material between the interfacial film and the formation of a multilayers reservoir that enables the changes in surface tension at the air-liquid interface.

PS consists primarily of phospholipids (primarily DPPC), with Surfactant Proteins A, B, C, and D contributing ~10% by weight³. These proteins are responsible for a variety of functions including the re-spreading of the surfactant with each respiratory cycle, assisting in surfactant multilayer formation and microbial clearance⁴. Surfactant Protein C (SP-C), integral to the physico-chemical properties of PS, has been shown to be directly involved in multilayer formation⁵.

High levels of cholesterol in PS are associated with life-threatening acute respiratory distress syndrome (ARDS) and acute lung injury (ALI)⁶. ALI is a complex inflammatory disease which results in the alveoli becoming flooded. In the past, the application of surfactant

therapy has been demonstrated to be ineffective for the treatment of ALI because, for amongst several reasons, the replacement surfactant is rendered dysfunctional by the excess cholesterol incurred during lung injury⁷.

Earlier, we and others showed that formation of multilayers in PS films under compression is a characteristic feature of functional surfactant^{8,9} and is greatly reduced by elevated cholesterol levels^{8,10}. In addition to inhibiting multilayer formation we showed that the presence of cholesterol at higher compressions (45mN/m) alters the lipid organization inducing small electrostatic domains¹¹ and reduces adhesive properties of the PS film¹².

Newer surfactant formulations, which contain higher concentrations of SP-C than previous formulations, have resulted in the reduction of ALI mortality¹³. The increased efficacy of these newer preparations is likely a result of SP-C's ability to mitigate the effects of high levels of cholesterol consistent with the *in vitro* research reported by Gomez-Gil¹⁴. For example, both Survanta and Curosurf have very little cholesterol while bovine lipid extract surfactant (BLES) has 2-5% and Infasurf and natural bovine surfactant have about 7% cholesterol¹⁵.

SP-C, integral to the physico-chemical properties of PS, and amyloid- β (1-40) (A β 40) share several similar properties including a mid-peptide "hinge" and their propensity to aggregate into amyloid fibrils. A β is a small 35-42 amino acid length peptide associated with Alzheimer's disease. In solution, A β appears primarily as a

random coil¹⁶. However, in the presence of lipids, monomeric A β has primarily two alpha helical secondary structures (amino acid sections 16-23 and 28-35) separated by a random coil hinge^{17,18}. A β has a propensity to misfold and aggregate to form amyloid fibrils, similar to SP-C¹⁹.

Earlier we showed that A β improves surface active properties of BLES surfactant²⁰, compromised by cholesterol. We demonstrated that addition of A β 40 to BLES film with 20% cholesterol restored multilayer formation in BLES films²⁰.

In this work we hypothesized that adhesion forces play an important factor in the formation and stability of the multilayers in PS films and studied the effect of cholesterol and A β on the adhesion properties of BLES films. Using atomic force spectroscopy (or force measurements), we show that the addition of A β 40 and cholesterol, separately, decreases the adhesive force of BLES. However, in BLES films already laden with 20% cholesterol, the addition of A β restores the adhesive force of BLES films. Based on this data and our earlier work²⁰ which showed a return of multi-layer formation with the addition of A β , we conclude that A β can restore the function of BLES counteracting the effect of cholesterol by improving adhesion properties of a BLES film.

Results and Discussion

We present force measurements on a BLES monolayer with and without 20% cholesterol and 10% A β 40 to elucidate the effect of cholesterol and A β on the tip-sample adhesion force and work of adhesion. Figure 1 shows representative AFM images of the supported BLES films created by the deposition of the four lipid-protein mixtures. A representative cross section is shown to demonstrate the profile of the surfactant film. Typical raw data force plots are shown in the bottom row of figure 1 corresponding to the AFM image displayed. These force plots demonstrate the difference in adhesion force and unbinding properties that were observed in the ensemble of force plots. While many force plots were collected and analyzed (~300 for each sample), the force plots in figure 1 are representative of those collected and serve as an example of typical force plots used for statistical analysis. The AFM force plot starts with the tip away from the surface. As the tip approaches the surface (x-axis), in red, a small negative force peak is observed. This small peak is the result of the tip suddenly bending and binding to the surface as a result of a variety of chemical (van der Waals, electrostatic, etc.) interactions. The tip continues to move towards the surface and the cantilever is bent as the tip is embedded in the lipid film. At this point, the tip retraction phase begins (blue line). The cantilever deflects as the tip remains bound to the surface. Suddenly, the tip-surface adhesion bonds rupture and the cantilever returns to a neutral position. This rupture event corresponds to the rupture peak observed below the baseline (fig 1 bottom). In addition to the adhesion force, we also measured the work of adhesion. The work of adhesion, W , is calculated by the data analysis software by taking the integral (i.e. area) of the force plot below the baseline. Work of adhesion is given by the equation:

$$W = \int F dz$$

BLES Control

Figure 1A shows an AFM image of a supported BLES monolayer without any additives deposited on mica at a compression of 35

mN/m. Typical liquid condensed phase domains, with a height of 0.4 nm above the liquid expanded phase base monolayer, were observed. At this lower compression, characteristic multilayer patches as reported earlier⁹ were not observed, and only the monolayer is present. These domains are predominately circular in shape as a result of surface energy minimization. The coexistence of larger domains (1995 \pm 283 nm) and smaller domains (107 \pm 14 nm) was observed on AFM images (fig 1A). The mean adhesion force was calculated as 22.1 \pm 1.28 nN. Glass, being harder than mica, had a mean adhesion force of 13.6 \pm 1.36 nN. From this data, and previously published work¹² we deduced that for the materials we investigated, softer materials are associated with higher adhesion forces. To probe the difference between liquid expanded phase and liquid condensed phase domains, we took force plots on both phases. We were able to determine the phase of the lipid being probed by using an AFM image of the lipid first and overlaying our force map on the AFM image. Given the presence of domains, we compared the adhesion forces seen on the domains to the adhesion forces seen on the underlying fluid phase lipid. Upon analysis of the force plots, there was no statistically discernible difference in unbinding forces taken from the liquid condensed domains as compared to unbinding forces taken from the underlying liquid expanded monolayer; the difference in mean adhesion force was within one standard deviation. We collected many AFM images to ensure that no multilayers were formed in the lipid films and to ensure that all force plots were taken on BLES monolayers.

BLES with 20% Cholesterol

Figure 1B shows an AFM image of BLES with 20% cholesterol. Previous research has shown that cholesterol stiffens BLES films and inhibits multilayer formation at higher compressions (45mN/m)^{8,12,20}. Our monolayer samples were prepared at lower compression (35 mN/m), and we also observed a decrease in adhesion forces with a mean adhesion force of 17.0 \pm 0.88 nN in cholesterol laden BLES samples as compared to pure BLES (22.1 \pm 1.28 nN) ($p < 0.01$).

At this compression, the monolayer appears smooth: only smaller domains are visible, but larger (micron-size) domains as observed in the BLES sample (Fig 1A) are no longer visible in the cholesterol-BLES monolayer (fig 1B).

BLES with 10% amyloid- β

Figure 1C shows an AFM image of supported BLES monolayer with 10% A β 40 deposited at a compression of 35 mN/m. Small circular domains similar to the small domains shown in the BLES image (fig 1A) appear, indicating that A β 40 does not affect domain formation as cholesterol does. Domains have sizes (231 \pm 10 nm). However, the mean adhesion force 14.7 \pm 0.83 nN was similar to the BLES film containing 20% cholesterol (17.0 \pm 0.88 nN) (fig 2), which is characteristic of a stiffened monolayer. The morphology of the force plot for the BLES-A β 40 sample is very sharp and the force distribution is narrow (fig 1 and fig 2) indicating a very sudden unbinding event characterized by much fewer lipid molecules being lifted off the surface compared to the cholesterol-BLES film.

BLES with 20% cholesterol and 10% amyloid- β

Figure 1D shows an AFM image of BLES with 20% cholesterol and 10% A β 40. We observed a return of domain formation: both larger (646 \pm 41 nm) and smaller (62 \pm 11 nm) domains were present, similar to what was observed in pure BLES sample (fig 1A). However, the most noticeable change was an increase in the adhesion force

compared to the BLES with 20% cholesterol sample. The mean adhesion force was 25.1 ± 1.43 nN - similar to the BLES control. With respect to the shape of the force plot, we observed a broad

unbinding event similar to that seen for the cholesterol sample (fig 1B).

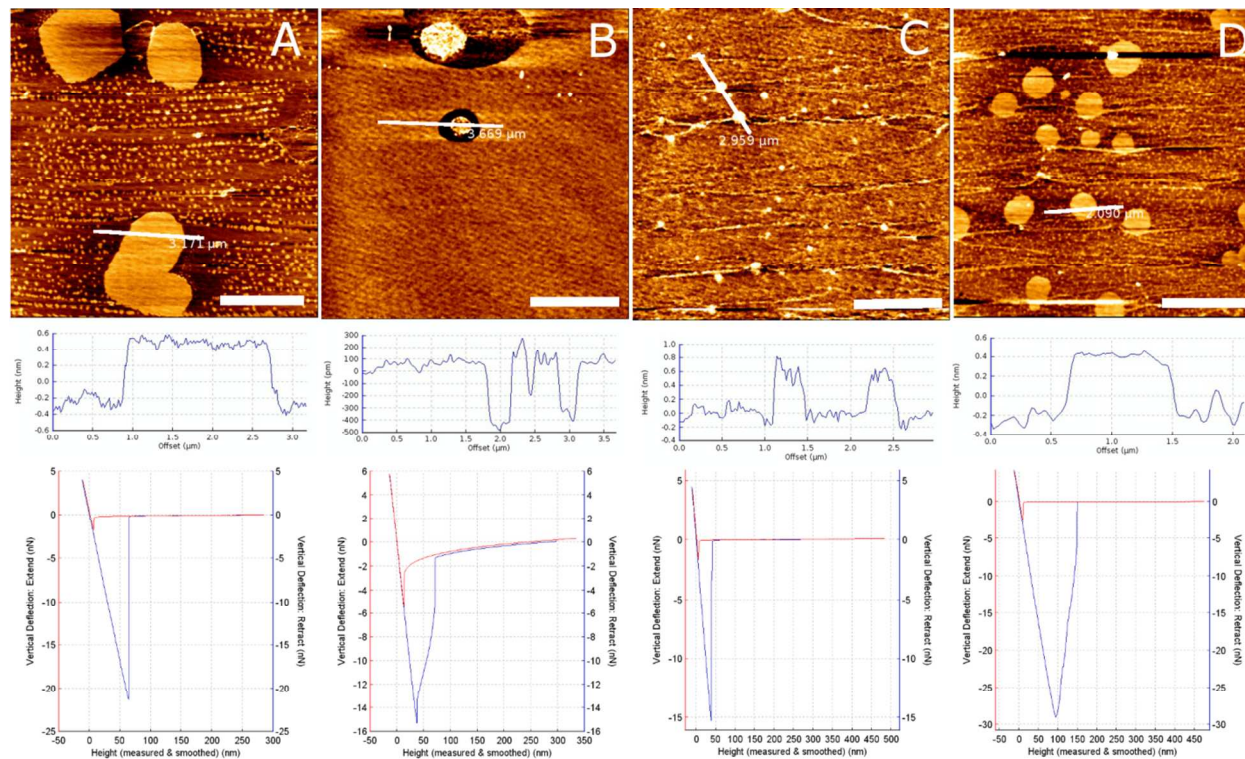


Fig. 1 – AFM images, cross sections and representative force plots (A) AFM image and cross section of BLES monolayer deposited on mica using Langmuir-Blodgett deposition at a compression of 35 mN/m (control) showing liquid condensed domains that have formed with a height of 0.5 nm. These domains are in a liquid condensed phase whereas the underlying monolayer is in a liquid-expanded phase. (B) AFM image and cross section of BLES monolayer with 20% cholesterol deposited on mica using Langmuir-Blodgett deposition at a compression of 35 mN/m showing a noticeable absence of the formation of any regular domains. (C) AFM image and cross section of BLES monolayer with 10% amyloid β deposited on mica using Langmuir-Blodgett deposition at a compression of 35 mN/m showing regular, albeit smaller domains than observed in the BLES control sample. (D) AFM image and cross section with 20% cholesterol and 10% A β 40 deposited on mica using Langmuir-Blodgett deposition at a compression of 35 mN/m showing the return of regular domains which were absent in monolayers with cholesterol and no A β 40. All scale bars are 2.5 μ m. Bottom row of images are representative force plots corresponding to AFM images above. The X axis represents the height above the sample in nm and the Y axis is the force on the cantilever in nN. The red trace represents the approach phase and the blue trace the retrace phase. As the cantilever approaches the surface, it suddenly deflects downwards and becomes attracted to the surface. As the cantilever is continually lowered, the cantilever begins to deflect until it reaches a predetermined set point indicated by the absolute maximum travel in the plot. At that point there is a pause followed by a retraction. As the trace passes through the X-axis, there is no more deflection on the cantilever. Below the X-axis, the cantilever is bound to the surface until the cantilever suddenly detaches from the surface. This force (absolute minimum) is referred to as the adhesion force.

Figure 2 displays adhesion force histograms for each BLES composition and figure 3 shows a statistical summary comparing the mean adhesion force, width of force plot, and the work of adhesion for the four BLES mixtures. The mean values were calculated from the entirety of the data set for each sample. As discussed above, adding cholesterol to BLES and adding A β 40 to BLES both result in lower adhesion force. The addition of both A β 40 and cholesterol to the BLES film resulted in a mean adhesion force which was similar to the BLES control.

We also analyzed the work of adhesion for all four samples (fig 3C). The work of adhesion is a function of both the adhesion force and the width of the force plot (i.e. the height at which the tip separates

from the sample). A higher work of adhesion, for an equal adhesion force, would imply that the force plot is wider and therefore the tip has attracted some of the lipid monolayer and lifted it a greater height above the substrate at the point of tip-surface separation. This increased distance of the dissociation between the tip and the sample may be the result of larger contact area and larger number of molecular interactions between the tip and the film. As shown in figure 3, the work of adhesion was slightly increased in BLES-cholesterol sample and decreased in BLES-A β 40 samples, but addition of both cholesterol and A β 40 led to an increase in both adhesion force and the work of adhesion as compared to pure BLES sample ($p < 0.01$).

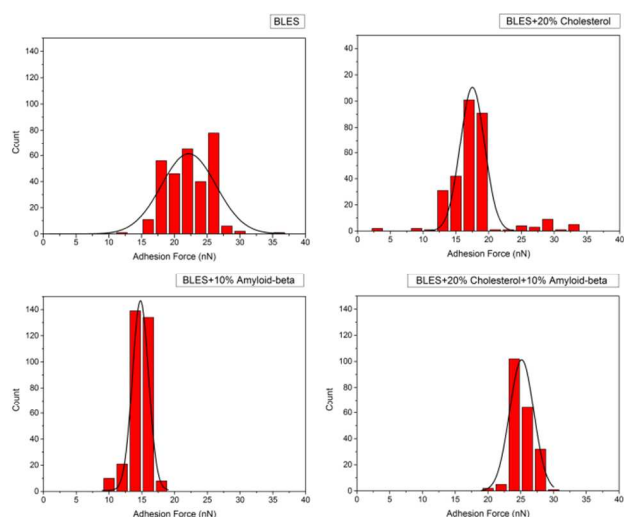


Fig. 2 – Adhesion force histograms of monolayer samples of BLES, BLES with 20% cholesterol, BLES with 10% A β 40 and BLES with 20% cholesterol and 10% A β 40. A Gaussian fit has been added to show the mean adhesion force of each mixture.

Discussion

Extensive research has been conducted on the effect of cholesterol on lipids^{21–36}. Of great interest to our current topic is cholesterol's complex and controversial effect on membrane fluidity. This effect is dependent on the lipid phase (characterized by phase transition temperature, T_m , which in turn is dependent on factors like lipid acyl chain length, degree of saturation, and head group): below the T_m , cholesterol increases membrane fluidity by interfering with the tight lipid packing associated with the gel phase (L_β)³³, and decreases membrane fluidity in liquid-crystalline phase (L_α) bilayers, such as DOPC, inducing an intermediate state, known as the “liquid ordered” phase³³.

Similar effects of cholesterol are observed in lipid-protein mixtures of PS films. The phase, or lipid order, for the monolayer at the air/water interface depends on the compression of the surfactant film: at lower compressions (such as studied here, 35mN/m), a monolayer exists in the L_α phase, while at higher compressions (40–45mN/m), a monolayer exists in the L_β phase. At compressions above 40 mN/m, functional PS film forms multilayers at the air/water interface^{8,37} (fig 4). Multilayer formation (and PS surface active properties) have been shown to be inhibited by elevated levels of cholesterol^{8,10}. In our previous report, we demonstrated that A β 40 improves multilayer formation counteracting the effect of cholesterol²⁰. Force measurements performed in this report clarified that A β 40 improves the adhesive properties of the monolayer, which may help to form and stabilize multilayer formations. Earlier work demonstrated that cholesterol reduces adhesion forces in BLES monolayers at higher compressions (45–47 mN/m)¹². In this work, we prepared monolayers at a lower compression (35 mN/m) which mimics the relaxed monolayer and the relaxed bilayer squeezed out of the monolayer (fig 4). A compression of approximately 30–35 mN/m is normally assumed for the model lipid bilayer³⁸. The BLES monolayer at this compression shows the co-existence of L_β and L_α domains (fig 1A). Inclusion of cholesterol slightly increases the lipid

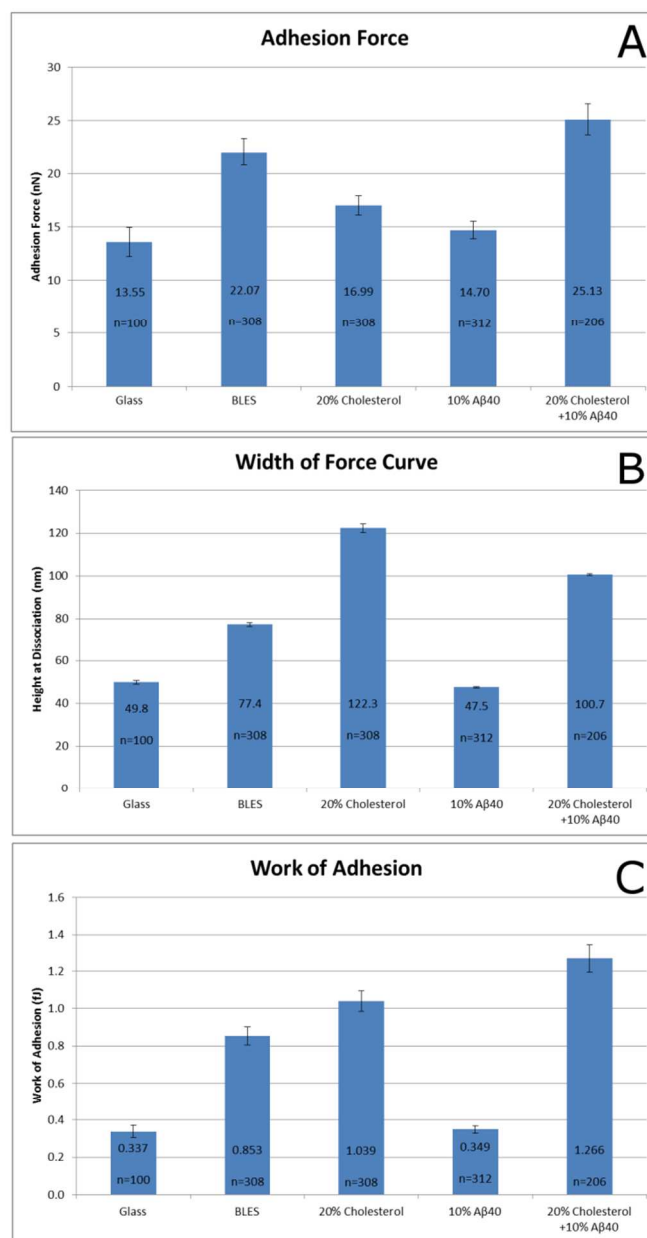


Fig. 3 – Comparison of Adhesion Forces, Width of Force Plot, and Work of Adhesion. Statistical means of adhesion force, (A), width of force plot, (B), and work of adhesion (C) measured on glass, BLES, BLES with 20% cholesterol, BLES with 10% A β 40 and BLES with 20% cholesterol and 10% A β 40. Error bars represent the estimate of standard error (standard deviation/ \sqrt{n}).

order in L_α domains which leads to a smoother appearance of PS film due to co-existence of L_β and liquid-ordered (L_o) domains, which are similar in height (fig 1B). This observation correlates with the well-known ordering effects of cholesterol, which result from increases in the ordering of the phospholipid hydrocarbon chains resulting in the formation of the L_o phase³⁹. This L_o phase is an intermediate state between what is referred to as a liquid crystalline-disordered phase (L_d) and L_β . The L_o phase requires the presence of cholesterol for its formation and is often studied in relation to lipid

rafts in systems usually consisting of cholesterol, sphingomyelin, and DOPC^{32,33}. The effect of cholesterol also broadens and eventually eliminates the L_{β} - L_{α} phase transition of phospholipid membranes^{32,40,41} which also occurs in phospholipid monolayers^{42,43}. A modification in lipid ordering is often accompanied by a change in domain formation which correlates with our data shown in figure 1. Cholesterol eliminates the differences between domains and decreases the domain size compared to BLES. When both A β 40 and cholesterol are present in BLES, larger domains reappear in the film and the film resembles a pure BLES monolayer where both larger and smaller domains are present (fig 1A&C). The dynamics and coexistence of various domains are important for PS function, as recent work by Zhang suggests that multilayer formation is initiated at the edge of domains¹⁵.

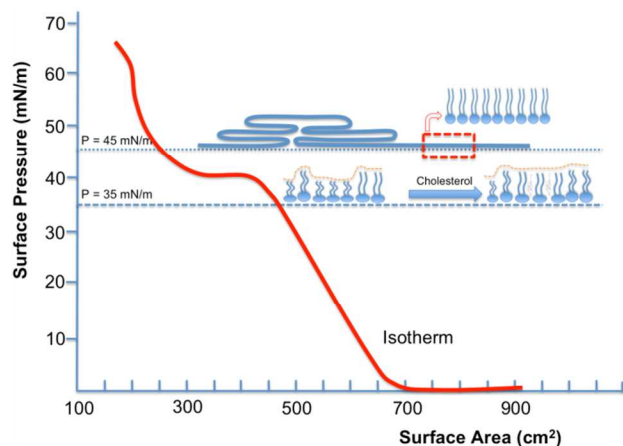


Fig. 4 – Schematic of Pulmonary Surfactant Phase Change and Multilayer Formation As PS is compressed, area per molecule decreases. Surface pressure, π , remains low as the lipid molecules remain in a gaseous phase. As surface area continues to decrease, surface pressure increases as the lipid molecules undergo a transition to the liquid condensed (gel) -liquid expanded (fluid) phase. The inhomogeneity between these two phases in the lipids is what causes lipid domains. The addition of cholesterol induces a phase transition towards the liquid condensed phase - an intermediate state known as the "liquid-ordered" phase". As the area/molecule continues to decrease, multilayers begin to form around 45 mN/m surface pressure. This corresponds to the brief "levelling off" of the isotherm, followed by an increase. Eventually, the isotherm levels off approaching 73 mN/m as the surface tension approaches 0. At this point surfactant material is lost from the surface into the subphase.

SP-C provides an important contribution to multilayer formation: SP-C has been shown to assist in multilayer formation by creating a link between the monolayer and bilayer¹⁹. The adhesion properties of the PS film itself are important as they may serve as an additional mechanism to stabilize and hold multilayers together. In this work we demonstrated that the adhesion force of BLES decreases with the addition of 20% cholesterol. This result correlates with the observed decrease in multilayer formation^{8,12,20} and decrease of adhesion force in BLES-cholesterol monolayers at higher compressions (45 mN/m). In contrast to the decreased adhesion force that cholesterol induces, we observed an increased work of adhesion in the presence of 20% cholesterol, which indicates that the contact area between the AFM tip (amount of molecules interacting with the AFM tip) may be larger in the presence of cholesterol as compared to pure BLES or BLES with A β 40. However, the greatest adhesion force and the

work of adhesion were observed when cholesterol and A β 40 were both present in the film (fig 3A and C).

Gomez-Gil et al.¹⁴ used Differential Scanning Calorimetry (DSC) to probe the thermodynamic properties of lipid films with cholesterol when SP-C is added, and showed that SP-C counteracts some of the deleterious effects of cholesterol on the lipid membrane. The authors attribute the observed phenomenon to the SP-C improving the mechano-elastic properties of the cholesterol laden lipid film. Considering the similarities between SP-C and A β 40, our results are consistent with the conclusions made by Gomez-Gil: we observe a change in the adhesion force when a similar peptide - A β - is added to the BLES-cholesterol film.

Ambroggio, et al.⁴⁴ studied the effect of A β on lipid mono- and bilayers and reported the molecular area of an A β molecule to be significantly larger than that of a lipid molecule. The authors suggested that A β directly interacts with the lipids altering the mechanical properties of the film and the cohesive properties amongst the lipid molecules. Their observations correlate with our observation that A β 40-BLES results in a reduced adhesion force compared to pure BLES films.

Previous research has shown that A β has a high affinity for cholesterol⁴⁵. As we discussed previously²⁰, the return of multilayer formation in BLES with cholesterol when A β 40 was added may be a result of the A β 40 binding to cholesterol and preventing cholesterol from exerting its stiffening effect on phospholipid bilayers. Similarly to A β 40, cholesterol may also directly interact with SP-C and may inhibit its function as a multilayer linker. When A β is present in the lipid film, it may absorb cholesterol molecules and decrease the interaction of cholesterol with SP-C. This hypothesis agrees with our force spectroscopy data: we observe that individually, both cholesterol and A β 40 appear to stiffen the BLES monolayer and reduce adhesion, but when present together they increase both the adhesion force and the work of adhesion, which, in turn may explain an improvement in the multilayer formation and PS surface active properties.

The addition of A β 40 to pulmonary surfactant formulations may have clinical relevance for the treatment of ARDS: since it has been established that an increase in surfactant cholesterol levels is associated with acute lung injury¹³, adding A β (or a synthetic peptide with similar structure) to a therapeutic surfactant may be a simple and low cost solution to "cancel out" the effects of cholesterol and may mitigate some of the effects associated with acute lung injury. A β 40 has a surprisingly similar structure to SP-C but has a propensity to misfold especially within the presence of lipids inducing additional oxidative stress. Our results demonstrate that a synthetic peptide, similar in structure to SP-C and A β 40, but without a propensity to misfold, may be an effective candidate for improving synthetic surfactant formulations.

Experimental Procedures

Bovine Lipid Extract Surfactant

Bovine Lipid Extract Surfactant (BLES), a kind gift of BLES Biochemicals Inc. (London, Canada), was received in an aqueous solution from the manufacturer at a concentration of 27 mg/mL. The BLES in aqueous solution was extracted into a chloroform solution using the Bligh-Dyer method⁴⁶. Briefly, 0.5 mL of BLES was placed in a centrifuge tube with 1 mL of methanol and 1 mL of chloroform.

The solution was centrifuged for 10 minutes at 5000 x g. The precipitate was removed and another 1 mL of methanol was added to the tube. The tube was centrifuged again for 10 minutes at 5000 x g. Again, the bottom phase was removed leaving BLES dissolved in chloroform. The Bligh-Dyer extraction method results in a surfactant concentration in chloroform identical to that of the surfactant concentration in the original aqueous solution^{8,10}.

Monolayer deposition using Langmuir Blodgett Trough

A total of 4 mixtures were made: pure BLES; BLES with 20% cholesterol by weight; BLES with 10% A β 40; and BLES with 20% cholesterol and 10% A β 40. Mixtures were prepared in chloroform as previously described²⁰. Approximately 5 μ L of chloroform solution was spread on the aqueous interface of the Langmuir-Blodgett trough and allowed to equilibrate for five minutes. The barriers of the trough were compressed at 20 mm/min until a surface pressure of 35 mN/m was reached. This surface pressure corresponds to the mean physiological surface pressure of pulmonary surfactant and is below the surface pressure where BLES monolayers have been shown to form multilayers²⁰. A 1 cm x 1 cm piece of freshly cleaved mica was raised through the interface and a monolayer of surfactant was collected on the mica at a constant compression of 35 mN/m. The mica was dried under a gentle nitrogen stream and stored in a desiccator until experiments were performed later the same day.

Atomic Force Microscopy

The JPK Nanowizard II atomic force microscope was used to collect AFM images of BLES monolayers supported on mica in intermittent contact mode in air, at a line rate 1 Hz. Bruker DNP cantilevers were used (spring constants 120-240 mN/m, resonance frequency 23-56 kHz). Images were processed using JPK SPM Data Processing Software v. 4.2.50. Images were flattened and z-ranges were adjusted to normalize features on all images.

Force Spectroscopy

A JPK Nanowizard II atomic force microscope was used for force measurements with a Bruker DNP cantilevers (spring constants 120-240 mN/m, resonance frequency 23-56 kHz). The AFM cantilevers were calibrated using the thermal noise method and cantilever spring constants were determined prior to the measurements on a glass slide in air. After calibration, the BLES monolayers were scanned in air at room temperature and at least 250 force plots were taken for each sample. Force plots were normalized and converted to force vs tip-sample separation plots. Analysis of the retraction part of the force plots was done using the JPK software in order to extract the adhesion force and work of adhesion (integral under the force plot). Statistical analysis was done to calculate the mean adhesion force and work of adhesion for each sample. Since the force plots were near triangular, the width of the force plot, (the height at which the tip dissociates from the lipid monolayer on the substrate), was approximated by dividing the area under the force plot (work of adhesion) by the height of the force plot (rupture force) and multiplying by two. The mean values and standard errors of these data are displayed in figure 3. Analysis of variance (ANOVA) ($\alpha=0.01$) was separately completed on the entirety of adhesion force ($F=530$) and work of adhesion ($F=218$) data points to determine that mean forces of adhesion were statistically significant. Following ANOVA, a *post hoc* Bonferroni test was applied to ensure that differences of data discussed were statistically significant⁴⁷. For all statements of comparison made in the text with regards to adhesion force, work of adhesion, and width of force plots, the differences are statistically significant, with $p<0.01$.

Conclusions

We demonstrated that the addition of A β 40 can ameliorate the detrimental effects of cholesterol in PS possibly by binding to cholesterol, effectively “cancelling out” the effect of cholesterol. Our results demonstrate that a synthetic peptide, similar in structure to SP-C and A β 40, may be an effective candidate for improving synthetic surfactant formulations.

Acknowledgements

Authors would like to thank BLES Biochemicals Ltd (London, ON) for their kind donation of BLES. The authors would like to thank Morgan Robinson for his critical reading of our manuscript and assistance with statistical analysis. The authors would like to thank a reviewer for their diligence in reviewing this report. This research was funded by Canadian Foundation for Innovation (CFI), Ontario Research Fund (ORF), and Natural Science and Engineering Council of Canada (NSERC), grants to ZL, an NSERC graduate scholarship and WIN Fellowship to ED.

Notes and references

^a Department of Biology

University of Waterloo
200 University Ave
Waterloo ON N2L 3G1 CANADA

^b Waterloo Institute for Nanotechnology

University of Waterloo
200 University Ave
Waterloo ON N2L 3G1 CANADA

^c Department of Physics and Astronomy

University of Waterloo
200 University Ave
Waterloo ON N2L 3G1 CANADA

† Corresponding author:

Zoya Leonenko
Department of Physics and Astronomy
University of Waterloo
200 University Ave
Waterloo ON N2L 3G1 CANADA
Email: zleonenk@uwaterloo.ca
phone (work): (519) 888-4567 ex 38273
fax: (519) 746-8115

Electronic Supplementary Information (ESI) available: [details of any supplementary information available should be included here]. See DOI: 10.1039/b000000x/

1. Y. Y. Zuo, R. Veldhuizen, W. Neumann, N. O. Petersen, and F. Possmayer, *Biochim. Biophys. Acta*, 2008, **1778**, 1947–1977.
2. S. Schürch, *Respir. Physiol.*, 1982, **48**, 339–355.
3. J. Goerke, *Biochim. Biophys. Acta*, 1998, **1408**, 79–89.
4. J. Pérez-Gil, *Biochim. Biophys. Acta*, 2008, **1778**, 1676–95.
5. J. Johansson, *Biochim. Biophys. Acta*, 1998, **1408**, 161–172.
6. A. Panda, K. Nag, R. Harbottle, K. Rodriguez-Capote, A. Ruud, W. Petersen, and O. Possmayer, *Am. J. Respir. Cell Mol. Biol.*, 2004, **30**, 641–650.
7. J. Lewis and R. Veldhuizen, *Annu. Rev. Physiol.*, 2003, **65**, 613–642.
8. Z. Leonenko, S. Gill, S. Baoukina, L. Monticelli, J. Doehner, F. Felderer, M. Rodenstein, L. M. Eng, and M. Amrein, *Biophys. J.*, 2007, **93**, 674–683.

9. A. von Nahmen, M. Schenk, M. Sieber, and M. Amrein, *Biophys. J.*, 1997, **72**, 463–9.
10. L. Gunasekara, S. Schürch, W. M. Schoel, K. Nag, Z. Leonenko, M. Haufs, and M. Amrein, *Biochim. Biophys. Acta*, 2005, **1737**, 27–35.
11. E. Finot, Y. Leonenko, B. Moores, L. Eng, M. Amrein, and Z. Leonenko, *Langmuir*, 2010, **26**, 1929–1935.
12. Z. Leonenko, E. Finot, V. Vassiliev, and M. Amrein, *Ultramicroscopy*, 2006, **106**, 687–694.
13. P. Markart, C. Ruppert, M. Wygrecka, T. Colaris, B. Dahal, H. Harbach, J. Wilhelm, W. Seeger, R. Schmidt, and A. Guenther, *Thorax*, 2007, **62**, 588–594.
14. L. Gomez-Gil, D. Schurich, E. Goormaghtigh, and J. Perez-Gil, *Biophys. J.*, 2009, **97**, 2736–2745.
15. H. Zhang, Y. E. Wang, Q. Fan, and Y. Y. Zuo, *Langmuir*, 2011, **27**, 8351–8358.
16. L. Hou, H. Shao, Z. Zhang, H. Li, N. Menon, E. Neuhaus, J. Brewer, I. Byeon, D. Ray, M. Vitek, T. Iwashita, R. Makula, A. Przybyla, and M. Zagorski, *J. Am. Chem. Soc.*, 2004, **126**, 1992–2005.
17. H. Shao, S. Jao, K. Ma, and M. Zagorski, *J. Mol. Biol.*, 1999, **285**, 755–773.
18. P. Faller and C. Hureau, *Dalt. Trans.*, 2009, **7**, 1080–1094.
19. J. Johansson, *Swiss Med. Wkly.*, 2003, **133**, 275–82.
20. F. Hane, E. Drolle, and Z. Leonenko, *Nanomedicine*, 2010, **6**, 808–14.
21. M. Bonn, S. Roke, O. Berg, L. Juurlink, A. Stamouli, and M. Muller, *J. Phys. Chem. B*, 2004, **108**, 19083–19085.
22. S. Chiu, E. Jakobson, R. Mashl, and H. Scott, *Biophys. J.*, 2002, **83**, 1842–1853.
23. R. De Almeida, A. Fedorov, and M. Prieto, *Biophys. journal2*, 2003, **85**, 2406–2416.
24. T. Harroun, J. Karsaras, and S. Wassall, *Biochemistry*, 2008, **47**, 7090–7096.
25. N. Kučerka, J. Pencer, M.-P. Nieh, and J. Katsaras, *Eur. Phys. J. E*, 2007, **23**, 247–254.
26. N. Kučerka, D. Marquardt, T. Harroun, M.-P. Nieh, S. Wassall, and J. Katsaras, *J. Am. Chem. Soc.*, 2009, **131**, 16358–16359.
27. J. Lemmich, K. Mortensen, J. H. Ipsen, T. Hønger, R. Bauer, and O. G. Mouritsen, *Eur. Biophys. J.*, 1997, **25**, 293–304.
28. D. Levy and K. Briggman, *Langmuir*, 2007, **23**, 7155–7161.
29. D. Lingwood and K. Simons, *Science*, 2010, **327**, 46–50.
30. S. J. Marrink, A. H. de Vries, T. A. Harroun, J. Katsaras, and W. S. R., *J. Am. Chem. Soc.*, 2008, **130**, 10–11.
31. H. Martinez-Seara, T. Róg, M. Karttunen, I. Vattulainen, and R. Reigada, *PLoS One*, 20105, **5**, e11162.
32. T. P. McMullen, R. N. Lewis, and R. N. McElhaney, *Curr. Opin. Colloid Interface Sci.*, 2004, **8**, 459–468.
33. H. Ohvo-Rekila, B. Ramstedt, P. Leppimaki, and P. Slotte, *Prog. Lipid Res.*, 2002, **41**, 66–97.
34. S. A. Pandit, S.-W. Chiu, E. Jakobson, A. Grama, and H. L. Scott, *Langmuir*, 2008, **24**, 6858–6865.
35. K. Simons and V. W. L. C., *Annu. Rev. Biophys. Biomol. Struct.*, 2004, **33**, 269–295.
36. E. Drolle, N. Kučerka, M. I. Hoopes, Y. Choi, J. Katsaras, M. Karttunen, and Z. Leonenko, *BBA - Biomembr.*, 2013, **1828**, 2247–2254.
37. M. Amrein, a von Nahmen, and M. Sieber, *Eur. Biophys. J.*, 1997, **26**, 349–57.
38. D. Marsh, *BBA - Biomembr.*, 1996, **1279**, 119–123.
39. H. McConnell and A. Radhakrishnan, *BBA - Biomembr.*, 2003, **1610**, 159–173.
40. R. A. Demel and B. De Kruff, *Biochim. Biophys. Acta*, 1976, **457**, 109–132.
41. M. Bonn, S. Roke, O. Berg, L. B. F. Juurlink, A. Stamouli, and M. Müller, *J. Phys. Chem. B*, 2004, **108**, 19083–19085.
42. J. Slotte, *Biochemistry*, 1992, **31**, 5472–5477.
43. P. Mattjus, R. Bittman, and J. Slotte, *Langmuir*, 1996, **12**, 1284–1290.
44. E. E. Ambroggio, D. H. Kim, F. Separovic, C. J. Barrow, K. J. Barnham, L. a Bagatolli, and G. D. Fidelio, *Biophys. J.*, 2005, **88**, 2706–13.
45. S.-R. Ji, Y. Wu, and S. Sui, *J. Biol. Chem.*, 2002, **277**, 6273–9.
46. E. Bligh and W. Dyer, *Can. J. Biochem. Physiol.*, 1959, **37**, 911–917.
47. R. Johnson, *Probability and Statistics for Engineers*, Pearson Education, Inc, Upper Saddle River, NJ, 7th edn., 2005.

